

Projection printing of gold micropatterns by photochemical decomposition

Thomas H. Baum, Ernesto E. Marinero, and Carol R. Jones

Citation: *Applied Physics Letters* **49**, 1213 (1986); doi: 10.1063/1.97418

View online: <http://dx.doi.org/10.1063/1.97418>

View Table of Contents: <http://scitation.aip.org/content/aip/journal/apl/49/18?ver=pdfcov>

Published by the [AIP Publishing](#)

Articles you may be interested in

[Directionally controlled transfer printing using micropatterned stamps](#)

Appl. Phys. Lett. **103**, 151607 (2013); 10.1063/1.4824976

[Low-cost x-ray mask based on micropattern sputtered lead film for x-ray lithography](#)

J. Vac. Sci. Technol. B **27**, 1299 (2009); 10.1116/1.3117259

[Molecular conductance measurements through printed Au nanodots](#)

Appl. Phys. Lett. **89**, 113107 (2006); 10.1063/1.2345613

[Micropatterning of metal films coated on polymer surfaces with epoxy mold and its application to organic field effect transistor fabrication](#)

Appl. Phys. Lett. **85**, 831 (2004); 10.1063/1.1776325

[Micropatterning of surfaces by excimer laser projection](#)

J. Vac. Sci. Technol. B **7**, 1064 (1989); 10.1116/1.584595



Projection printing of gold micropatterns by photochemical decomposition

Thomas H. Baum and Ernesto E. Marinero

IBM Almaden Research Center, 650 Harry Road, San Jose, California 95120-6099

Carol R. Jones

IBM General Technology Division, 1701 North Street, Endicott, New York 13760

(Received 23 June 1986; accepted for publication 9 September 1986)

Gold micropatterns have been generated by the laser photolysis of dimethylgold (III) acetylacetonate, $\text{Me}_2\text{Au}(\text{acac})$, in the vapor phase. Linewidths as fine as $2\ \mu\text{m}$ were readily obtained utilizing a simple optical projection system comprised of a $4\times$ projection lens, a lithographic photomask, and the UV output from an excimer laser. The single-step, dry process for selectively producing metal patterns is highlighted.

The fabrication of metallic patterns plays an essential role in the microelectronics industry today. At present, the selective definition of metal for circuitization relies upon a series of complex lithographic processes.¹ These techniques are time consuming and are dependent upon the use of several development steps. A simpler approach to the generation of metal patterns would be of great scientific and economic significance.

In recent years, the utilization of lasers to induce chemical reactions has gained considerable attention; the ability to selectively deposit and/or etch materials has been reviewed.² The potential of this approach has far-reaching implications for circuitization, line repair, and mask repair. Laser-induced chemical reactions are simple, direct processes which avoid the need for solvents and lithography. The degree of spatial resolution achievable with lasers allows fine dimensions to be realized. At the same time, the availability of large beam, excimer lasers allows large areas with fine features to be processed as well.

Recent work from this laboratory has explored laser-induced deposition of gold³ and copper⁴ from metal acetylacetonate complexes. Both pyrolytic and photolytic techniques of deposition have been achieved. Although it has been proposed⁵ that full microcircuits can be deposited by a serial pyrolytic process, this requires fast "writing" rates and long processing times. An alternate approach has been realized in this work: the selective patterning of gold films from the vapor phase photolysis of dimethylgold (III) acetylacetonate, $\text{Me}_2\text{Au}(\text{acac})$, complex. The utility of excimer lasers for projection printing of lithographic materials has been demonstrated⁶ and can be extended to vapor phase metal deposition.

In this preliminary work, we have set out to determine the feasibility of the method, the line resolution and film properties generated by UV photolysis. The dimensions of the deposit were defined by a lithographic mask after a $4\times$ reduction by an optical lens setup. The laser wavelength was selected so that it was absorbed by the volatile gold complex, thus resulting in photodecomposition to metal. The general experimental apparatus and approach, as well as our preliminary findings, are described.

The gold complex utilized throughout this study was synthesized according to the literature procedure of Brain and Gibson.⁷ Tetrachloroauric acid was commercially avail-

able (Aldrich Chemical Co.) and was the starting material in the synthesis. The final product, $\text{Me}_2\text{Au}(\text{acac})$, was purified by sequential sublimations to yield long, white needles of crystalline product ($\text{mp} = 82^\circ\text{C}$). The room-temperature vapor pressure of the complex is approximately 9 mTorr. A vapor phase spectrum was obtained on a Beckman spectrophotometer (model DU-8) with a 5-cm path length quartz cell; λ_{max} at 203 and 305 nm with shoulders at 265 and 330 nm.

Micropatterns were generated through the use of the experimental apparatus shown schematically in Fig. 1. A chrome-on-quartz lithographic mask was utilized to define the photoimage. The projected pattern was subsequently reduced by a projection lens system⁸ with a calculated resolution of $2\ \mu\text{m}$ on axis. In practice, the mask to lens distance was altered to achieve a $4\times$ reduction of the pattern; the focal plane was located experimentally by ablative photodecomposition⁹ of a polymer on silicon wafers. The projected pattern was optically inspected to find the best overall resolution versus distance from the lens setup. At best focus, a $1.0\times 1.0\ \text{cm}^2$ pattern is converted to a $0.25\times 0.25\ \text{cm}^2$ patterned image with a focal distance of 22.7 mm. The overall transmission of the lens setup is 62% and the focal plane distance was re-optimized for each UV wavelength utilized.

Two commercial excimer lasers provided the ultraviolet radiation: A Lumonics TE-860-3 was operated with XeCl (308 nm) and a Lambda Physik EMG-102 excimer was operated with ArF (193 nm) and KrF (248 nm). Both lasers produced rectangular beams of $25\times 12\ \text{mm}$. The intensity distribution across the beam profile is inhomogeneous and was apertured to 1 cm to minimize the spatial intensity inhomogeneity. The laser beam energy was monitored with a joulemeter.

The deposition cell consisted of a four-way stainless-steel cross equipped with a vacuum valve, quartz windows, and a metal ampoule containing the gold complex. The organometallic was degassed prior to irradiation by several freeze-pump-thaw cycles in liquid nitrogen. The micropattern images were projected onto the inside surface of the front window of the cell which was located at the optimum focal plane. After deposition, the windows could be removed to allow inspection and analysis of the metal patterns.

Films were examined optically and by scanning electron microscopy (SEM-Philips 505). Film thickness was mea-

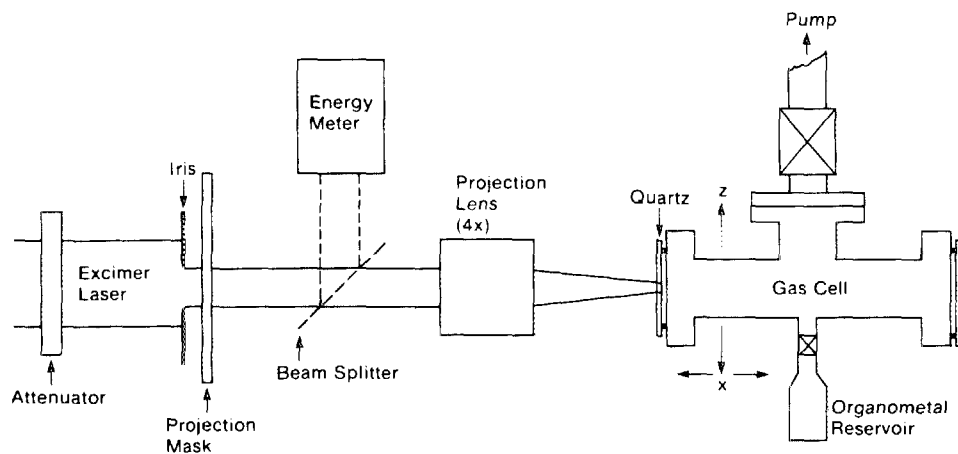


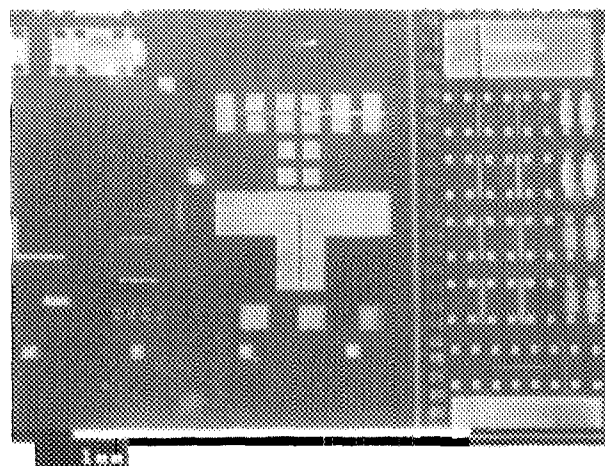
FIG. 1. Schematic diagram of the experimental setup utilized in this study.

sured by a Tencor Instruments Alpha-Step profilometer and adhesion was qualitatively examined with adhesive tape. Film purity was examined with a Hewlett-Packard ESCA spectrometer (model 5950B) equipped with an Al $K\alpha$ x-ray source (1487 eV) and a monochromator for enhanced emission resolution. The deposits were argon ion depth profiled and charging of the quartz substrates was eliminated with a 0.1 mA flood gun emission current during the analyses. Scofield cross sections¹⁰ were utilized to correct for the sensitivities of the individual elements after calibration to an evaporated gold standard. Atomic percentages were calculated by a first-order approximation and are listed in Table I.

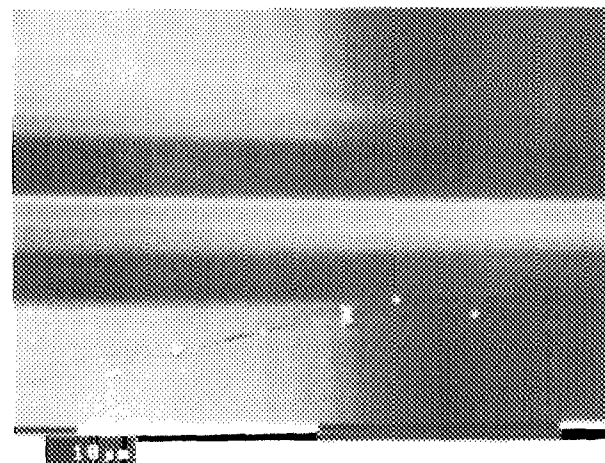
A gold pattern was generated [Fig. 2(a)] by the vapor phase photolysis of $\text{Me}_2\text{Au}(\text{acac})$ using the experimental setup in Fig. 1 with 1000 pulses of 248 nm radiation. The total laser fluence at the quartz window is calculated to be 618 J/cm^2 . The film thickness is uniform across the pattern with an average height of $0.2 \mu\text{m}$. SEM examination of the pattern revealed that $2 \mu\text{m}$ line and space resolution [Fig. 2(b)] was cleanly achieved. Although $1 \mu\text{m}$ features were produced in the ablated polymer (focal plane optimization) with a single pulse, these are not resolved in the gold photo-deposit. Further experimentation is required to evaluate the source of the image degradation in the gold deposits; multiple laser exposures, instabilities in the optical setup, or the photoprocess itself may be responsible.

The quality of the deposited material was explored and atomic percentages, determined by x-ray photoelectron spectroscopy, are listed in Table I. A compositional variation of the deposited material was observed versus the laser

wavelength utilized. The highest gold content was observed at 248 nm, while both 193 and 308 nm radiations produced photodeposits with greater contamination. The vapor phase UV spectrum of the organogold complex exhibits a mini-



(a)



(b)

FIG. 2. SEM photographs of a gold pattern deposited by vapor phase photolysis. (a) Portion of patterned gold deposit; (b) close-up showing $2 \mu\text{m}$ line and space resolution in the same pattern.

TABLE I. X-ray photoelectron spectroscopic analysis of photodeposited films. Films were produced with 24 mJ/pulse average power.

Wavelength	No. of pulses	Au	C	O
308	18 000	28	59	13
308	20 000	28	58	14
248	18 000	76	11	13
248	20 000	52	43	5
193	18 000	23	73	4
193	20 000	25	68	7
254	(lamp)	78	22	0

mum in absorption at 248 nm, in comparison to 193 and 308. Yet this is precisely the wavelength that provides a photodeposit with the highest purity. This wavelength dependence may be related to different primary dissociative pathways, different electronic states, or from secondary photoreactions of the primary photoproducts. Interestingly, the photodeposits were found to be quite adherent and survived several adhesive tape pulls without damage. This result is in direct contrast to that observed for evaporated films on quartz. As might be expected, the sheet resistivities of the deposits were several orders of magnitude higher than bulk metal due to the high carbon contamination. However, a post-annealing step showed marked reductions in the electrical resistances.

The general approach utilized in this study creates an inherent limit to the film thicknesses produced. As the gold photodeposit grows, the reflectivity and absorptivity of the film increase for the wavelengths used; thus, later incoming pulses are attenuated. The rate of deposition is observed to decrease with attenuation of the incident radiation and the film thickness becomes self-limiting. Films of 2000–3000 Å could be produced, but thicker films were not obtained under these experimental conditions. Furthermore, at high laser fluences, ablation of the growing photodeposit has been observed.

Several thin films of gold were evaporated onto quartz wafers and their transmission spectra in the UV were examined. No significant differences in transmission were observed for the films at 193, 248, or 308 nm, independent of the thickness. This rules out the possibility that one wavelength may be more highly absorbed by the growing film from later pulses of radiation. Also, an irradiation with 351 nm (XeF) light did not induce photodecomposition or gold deposition. This wavelength is very weakly absorbed by the complex and indicates that no thermal process is initially important for deposition. With the quartz windows being transparent to all the wavelengths used, the primary mode for decomposition is photochemical in nature. However, the latter pulses of UV may be absorbed by the growing film and introduce a thermal component to deposition. The thermal decomposition of $\text{Me}_2\text{Au}(\text{acac})$ has been shown¹¹ to produce high quality gold; thus, the thermal component would appear to be small based upon the XPS data.

The primary impurity in all the deposited films is carbon; the oxygen content in these films represents an upper limit due to the high content of oxygen in the exposed areas of the quartz substrate. The carbon impurity is most likely not trapped starting complex due to the ratio of the elements. The starting gold complex has a C/Au ratio of 7, yet much lower ratios of C/Au are observed in the films. This argues for a decomposition pathway by which carbonaceous impurities are trapped in the growing films; secondary photolysis of photoproducts or surface adsorbed species seems likely.

In these experiments, the initial deposition of gold is solely photochemical in nature. The observed wavelength dependence cannot be explained by a thermal mechanism. Also, in separate experiments we have demonstrated the photodecomposition of $\text{Me}_2\text{Au}(\text{acac})$ with a low pressure, mercury arc lamp (254 nm). In these experiments, there is no significant temperature rise; deposition of a golden image was observed and contained a C/Au ratio of 0.28 by XPS. Transmission electron microscopy (TEM) was used to examine a photodeposit produced by lamp irradiation under similar experimental conditions to the excimer depositions. The observed TEM is similar to that produced by a heterogeneous evaporation.¹² Assuming a commonality with evaporated metals, these results are indicative of crystal formation via surface nucleation and condensation of vapor phase gold particles to form crystalline aggregates. The crystallinity of the gold particles was confirmed by x-ray diffraction.

The vapor phase deposition of gold films has been demonstrated by UV laser projection printing. In general, the process shows great potential for the selective patterning of thin metal films. Gold films deposited in this fashion are contaminated with carbon impurities and further studies will try to better understand the overall photochemistry of $\text{Me}_2\text{Au}(\text{acac})$. The demonstrated method has a high degree of spatial resolution and metal images can be produced rapidly. A basic understanding of the photochemistry of selected organometallics may help to produce higher quality metal films by this method.

The authors are grateful to V. Hanchett for the TEM results.

¹For a general review, see L. F. Thompson, C. G. Willson, and M. J. Bowden, eds., *Introduction to Microlithography*, ACS Symposium Series (American Chemical Society, Washington, DC, 1983).

²D. J. Ehrlich and J. Y. Tsao, *J. Vac. Sci. Technol. B* **1**, 923 (1983).

³T. H. Baum and C. R. Jones, *Appl. Phys. Lett.* **47**, 538 (1985).

⁴C. R. Jones, F. A. Houle, C. A. Kovac, and T. H. Baum, *Appl. Phys. Lett.* **46**, 204 (1985); F. A. Houle, C. R. Jones, T. Baum, C. Pico, and C. Kovac, *Appl. Phys. Lett.* **46**, 1 (1985); C. R. Moylan, T. H. Baum, and C. R. Jones, *Appl. Phys. A* **40**, 1 (1986).

⁵I. P. Herman, B. M. McWilliams, F. Militzky, H. W. Chin, R. A. Hyde, and L. L. Wood, *Laser Controlled Chemical Processing of Surfaces*, MRS Symposium, **29**, 29 (Elsevier, New York, 1984).

⁶K. Jain and R. T. Kerth, *Appl. Opt.* **23**, 648 (1984).

⁷F. H. Brain and C. S. Gibson, *J. Chem. Soc.* 762 (1939).

⁸M. Latta, R. Moore, S. Rice, and K. Jain, *J. Appl. Phys.* **56**, 586 (1984).

⁹R. Srinivasan, *J. Vac. Sci. Technol. B* **1**, 923 (1983); R. Srinivasan and W. Leigh, *J. Am. Chem. Soc.* **104**, 6748 (1982); and Refs. 6 and 8.

¹⁰J. H. Scofield, *J. Electron Spectrosc.* **8**, 129 (1976).

¹¹T. H. Baum and C. R. Jones, *J. Vac. Sci. Technol. B* **4**, 1187 (1986) and Ref. 3.

¹²A. Renou and M. Gillet, *J. Cryst. Growth* **44**, 190 (1978).